NASA/CR—2000-210369

Oxidation Behavior of GRCop-84 (Cu-8Cr-4Nb) at Intermediate and High Temperatures

Linus U. Thomas-Ogbuji and Donald L. Humphrey
Dynacs Engineering Company, Inc., Brook Park, Ohio

Prepared under Contract NAS3–98008

National Aeronautics and
Space Administration

Glenn Research Center

August 2000

Acknowledgments

The assistance of the following persons is gratefully acknowledged: D.L. Ellis of CWRU (with samples and properties information); T.R. McCue of Dynacs Engineering Company, Inc. (SEM/EDS); R.G. Garlick of NASA GRC (XRD); and D.J. Keller of RealWorld Quality Systems (statistical analyses).

This report contains preliminary findings, subject to revision as analysis proceeds.

Available from

NASA Center for Aerospace Information
7121 Standard Drive
Hanover, MD 21076
Price Code: A03

National Technical Information Service
5285 Port Royal Road
Springfield, VA 22100
Price Code: A03

Available electronically at http://gltrs.grc.nasa.gov/GLTRS

OXIDATION BEHAVIOR OF GRCop-84 (Cu-8Cr-4Nb) AT INTERMEDIATE AND HIGH TEMPERATURES

Linus U. Thomas-Ogbuji and Donald L. Humphrey
Dynacs Engineering Company, Inc.
Brook Park, Ohio 44142

SUMMARY

The oxidation behavior of GRCop-84 (Cu-8 at%Cr-4 at%Nb) has been investigated in air and in oxygen, for durations of 0.5 to 50 hr and temperatures ranging from 500 to 900 °C. For comparison, data was also obtained for the oxidation of Cu and NARloy-Z (Cu-3 wt% Ag-0.5 wt% Zr) under the same conditions. Arrhenius plots of those data showed that all three materials had similar oxidation rates at high temperatures (≥750 °C). However, at intermediate temperatures (500 to 750 °C) GRCop exhibited significantly higher oxidation resistance than Cu and NARloy-Z. The oxidation kinetics of GRCop-84 exhibited a sharp and discontinuous jump between the two regimes. Also, in the high temperature regime GRCop-84 oxidation rate was found to change from a high initial value to a significantly smaller terminal value at each temperature, with progress of oxidation; the two different oxidation rates were found to correlate with a porous initial oxide and a dense final oxide, respectively.

INTRODUCTION

GRCop-84 is a Cu-Cr-Nb alloy in which a bimodal dispersion of highly stable Cr_2Nb particles strengthen a matrix that is essentially pure Cu. Developed at the NASA Glenn Research Center and Case Western Reserve University (CWRU), this alloy has excellent properties that make it a strong candidate for applications where the retention of high strength and high conductivity at elevated temperatures are important. Chief among those applications are rocket nozzles and combustion chamber liner for reusable launch vehicles (RLV), the planned successors to the current NASA space shuttle. Accounts of the mechanical and thermophysical properties of this alloy may be found elsewhere (refs. 1 to 4), and it is to be noted that those properties are not significantly degraded by prolonged exposures at high temperatures—for durations that exceed expected lifetimes in service, at temperatures close to the alloy melting point (refs. 3 and 5).

However, little is known about the oxidative behavior of this alloy. An RLV combustor liner is expected to operate under conditions ranging from cryogenic temperatures to the vicinity of 800 °C (ref. 6). It is known that copper alloys are prone to serious degradation by blanching, as well as rapid oxidation, in such environments. Blanching, an occurrence in engine conditions characterized by oxidizing-to-reducing oscillation in the local ambient, has been the subject of several investigations (refs. 7 to 9), including studies now underway at NASA-GRC. However, the oxidation behavior of GRCop-84 is unknown, and remains an issue because rapid oxidation kinetics are known to be a major impediment to the use of copper-based materials in oxidizing environments at high temperatures (ref. 10). Our ongoing studies of oxidative degradation modes in GRCop-84 are intended to provide insight into both blanching and oxidation behavior, including oxidation kinetics and their relation to oxide compositions and morphologies. The service environment in an RLV engine will, of course, be far from isothermal or static. Nevertheless, oxidation experiments in such quasi-static conditions can provide valuable baseline data for modeling, design, and materials selection. It is pertinent to determine how the oxidation resistance of GRCop-84 compares with those of two other, related materials: pure copper (which is the matrix and major phase in this alloy) and NARloy-Z (Cu-3 wt%Ag-0.5 wt% Zr), which is presently in use as a liner material for the space shuttle main engine. This report presents, for comparison, our results for these three materials.

PROCEDURE

Extruded rods of GRCop-84, as well as wrought bars of NARloy-Z and oxygen-free, high-conductivity (OFHC) copper, were supplied by D.L. Ellis of CWRU. The samples were cut into coupons, drilled with hang-holes, and polished to 1000-grit finish. The oxidation experiments were performed in thermogravimetric analysers (TGA) fitted with *Cahn-1000* microbalances. The coupons of copper, NARloy-Z, and GRCop-84 were exposed to air or oxygen

at 100 standard cubic centimeters per minute (sccm) from 500 to 850 °C. Oxidation temperatures were initially set 100 °C apart; however, but this was reduced first to 50 °C and later to 25 °C intervals for GRCop-84, due to significant changes in oxidation behavior observed at the different temperatures. Morphology of the oxide scale was examined by SEM, distribution of constituent elements by EDS, and phase composition by XRD. In each case the examination covered the top surface of the oxide scale (oxide/gas interface), the oxide cross-section exposed by fracture, and the bottom surface of the oxide (oxide/alloy interface); in some cases it included elemental profiles of the alloy constituents in the metal just under the oxide.

RESULTS

Figure 1(a) is an Arrhenius plot (logarithm of parabolic rate constant, k_p, versus the inverse of oxidation temperature) for Cu oxidation in O_2; a similar plot from the literature on Cu oxidation (ref. 11) is reproduced in figure 1(b) for comparison. (Note, however, that fig. 1(b) was obtained from 8-hr oxidation experiments; in the present study oxidation durations were 50 hr.) Figure 1(a) exhibits two kinetic regimes between 500 and 900 °C; figure 1(b) shows the same, as well as a third regime below 450 °C. (The experiments reported here did not cover temperatures below 500 °C.) Figure 1(a) indicates an activation energy of 1.55 eV (~150 kJ/mol) for the high temperature oxidation of Cu and 0.88 eV (~85 kJ/mol) for intermediate temperatures; figure 1(b) indicates activation energies of 1.75 eV (170 kJ/mol) and 0.87 eV for the same respective regimes. (Figure 1(a) has been rendered in the same scale and units as fig. 1(b) for comparability; all other plots are in SI units.) Thus, except for minor disagreements (~50 °C difference in the point of transition from intermediate to high regimes of temperature, and a 10 percent difference in the activation energy for the high-temperature regime), the two plots are in very good agreement.

Figure 2 shows the results obtained for the oxidation of GRCop-84 in oxygen at the various temperatures, co-plotted with the Cu data already seen in figure 1(a), with the least-squares regression lines for different regimes of interest indicated. At intermediate temperatures (below ~700 °C) parabolic rate constants for GRCop-84 oxidation are significantly lower than those of copper (by up to an order of magnitude), whereas in the high-temperature regime the oxidation rates of the two materials are comparable.

In the regime of transition to high-temperature behavior (i.e., the interval 700 to 750 °C), the "parabolic" kinetic plot of the data became very wavy. This is shown in figure 3, where it may be seen that the waviness was closely reproducible with repeat runs. Reproducibility is evident in the near coincidence of the curves in figure 3 and in similar k_p values obtained for repeat runs at various temperatures (fig. 2).

In the high-temperature regime the oxidation of GRCop-84 started at a fast rate but ended at a slower rate. Figure 4 is a parabolic plot of the data for oxidation at 800 °C; it illustrates the decline of kinetics with progress of oxidation. Detailed statistical analyses of the data confirmed that the difference between the initial- and final-stage slopes was significant at the 99.9 percent confidence level. The initial stage (of high k_p) lasted 2 to 10 hr, while final stage (of lower k_p) occupied the last 30 to 40 hr of oxidation. With increase in oxidation temperature the initial stage duration became shorter, and the terminal stage longer. This bifurcation of kinetics is demonstrated in figure 2 by two branches of the Arrhenius slope, labeled #4 (faster, initial stage) and #5 (slower, final stage). The ratio of k_p values for the two stages, $(k_p)_i/(k_p)_f$, averaged ~3.0 for 25 runs between 775 and 900 °C: 5 runs each at 800, 825, and 850 °C and 3 each at 775, 875 and 900 °C. In contrast, Cu showed no such bifurcation, exhibiting only one slope to the Arrhenius plot in each temperature regime. The activation energy for initial-stage oxidation of GRCop-84 at high temperatures (slope #4) is the same as for Cu oxidation in the same temperature regime (slope #3). However, the activation energy for terminal-stage oxidation of GRCop-84 at high temperatures (slope #5), appears to be somewhat smaller, and also to coincide with those for Cu and GRCop-84 oxidation at intermediate temperatures (slopes #1 and 2).

Figure 5 compares the oxidation of GRCop-84 in air and in oxygen. The oxidation rates and trends are essentially the same in air and O_2, including the significant jump in k_p between the intermediate and high-temperature regimes. (The bifurcation of rate constants at high temperatures, illustrated in fig. 2, was suppressed in fig. 5, in the interest of clarity, by averaging the two k_p values for each temperature.) It is not surprising that oxidation rates for a copper alloy would be the same in air and oxygen, even though O_2 partial pressures differ by a factor of five in the two cases. The rate-limiting event in the oxidation of Cu alloys to Cu_2O/Cu is out-diffusion of Cu ions through the Cu_2O layer to the oxide-gas interface, which is not sensitive to $p(O_2)$ under the conditions of this study (ref. 11).

Figure 6(a) compares the oxidation rates of GRCop-84 and NARloy-Z in air, while figure 6(b) compares the oxidation behavior of the two materials in oxygen—with Cu included for reference. The TGA data for both

materials were derived from *thick coupons*, but those labeled NARloy-Z "wt. change" in the legend of figure 6(a) are unpublished data supplied by K.T. Chiang of *Rocketdyne* from oxidation experiments on NARloy-Z *wafers* in air. The data for NARloy-Z oxidation in air did not show the same, good reproducibility observed for NARloy-Z in oxygen and for GRCop-84 in both oxygen and air. Clearly any difference between the two materials with respect to oxidation in air is indistinguishable from data scatter. In oxygen, however, major differences appear, as may be seen in figure 6(b): At high temperatures the three materials have essentially the same oxidation rates in oxygen (as they do in air). But at intermediate temperatures GRCop-84 exhibits markedly lower oxidation rates than either NARloy-Z or Cu.

The SEM image in figure 7 shows a cross-section of the oxide scale grown on GRCop-84, in oxygen, at 550 °C. In all GRCop-84 samples the oxide scales were found to have only two compositional strata: an inner scale of Cu_2O and an outer layer of CuO—the former being ~20 times thicker than the latter on average. The oxide top surface exhibited the hallmark CuO whiskers, which were in profusion at lower temperatures but very sparse at high temperatures. However, the most striking feature observed was the existence of two morphological zones in the oxide scale, as may be seen in figure 7. The inner zone to the right represents early-stage oxide, while the outer zone at the left is terminal-stage oxide. The outer oxide is dense Cu_2O with a skin of CuO, and the inner oxide is spongy (highly porous) Cu_2O with trace amounts of Cr and Nb oxides (see below). EDS elemental maps of the entire oxide scale are shown below the SEM image in figure 7, while figure 8 shows EDS spectra from zones correspondingly labeled in the image of figure 7: zone A being the porous inner oxide and zone D the dense outer oxide. The map and spectra agree on all features: O and Cu are uniformly distributed across the oxide scale, while Cr and Nb are present in the inner oxide but absent from the outer oxide. The progressive depletion of Cr and Nb with maturity and increasing density of the oxide is clear in figure 8.

Only the two oxides of copper formed continuous layers at any temperature studied; other oxides were detected by XRD but were not observed as continuous layers. Table I gives a summary of the various oxides identified, or strongly indicated (with insufficient peak intensities for positive identification), in the oxide scales. The minor oxides were located at the oxide/metal interface and in minute quantities. Not only were their respective peaks weak, but they could not be detected by XRD scans from the tops of even the thinnest oxide films; they were detected only by lifting the oxide and scanning its underside. CrO_2 was usually present, but in even smaller quantities than binary oxides of Cu, Cr, and Nb, and combinations thereof. Table II lists XRD results for a set of samples oxidized for 0.5 to 5.0 hrs at 800 °C (to ascertain the sequence of formation of the oxides). It is evident that all the oxides detected in the mature scales (table I) were also present in the nascent oxide films (table II). In other words, a wide range of oxides was present from the start, and that situation did not change with duration or temperature of oxidation.

DISCUSSION

The good agreement in figure 1 between the present results and the literature values for Cu oxidation makes it possible to distinguish, in figure 2, between features that are attributable to Cu oxidation and those that are not. Clearly, the continuous and discontinuous changes in oxidation resistance of GRCop-84 are real. There is a major difference between the oxidation rates of GRCop-84 at intermediate and high temperatures, the cause of which is as yet unknown. The other significant difference is between the initial and terminal rates of GRCop-84 oxidation at high temperatures. While it is smaller, it is nonetheless real (as confirmed by rigorous statistical analyses). It coincides with, and probably arises from, the different oxide morphologies in those two stages. Different morphologies may also explain the apparently different activation energies for oxide growth in those two stages (as evidenced in slopes #4 and #5 in fig. 2). While the difference in activation energy is slight, it hints at some subtle shift in mechanism or rate-limiting step. It may reflect the effects of oxide densification and coarsening with prolonged dwell at high temperatures. Such ripening of the oxide is known to affect diffusion kinetics, for instance by reducing contributions from surface and grain boundary diffusion in the oxide (ref. 11).

The wavy kinetic curves in the transition temperature range (fig. 3) may be an indication of competing mechanisms, since parabolic, cubic, and logarithmic kinetics have all been reported for Cu_2O/CuO formers in that temperature range (ref. 12). On the other hand, it may suggest an oscillation between fast and slow oxidation rates driven by changes in oxide morphology, since the two morphologies were observed in varying proportions at all the temperatures studied. The two effects are not mutually exclusive; both may be present. Figure 7 shows a clear correlation between initial and terminal oxidation kinetics on one hand, and the dissimilar oxide morphologies in those two oxidation stages on the other hand. The dense, outer scale corresponds to the slower terminal-stage

oxidation and the porous inner oxide to the fast, early-stage oxidation. The early oxidation proceeds 3 times faster than the terminal stage because the highly porous initial oxide constitutes a less efficient diffusion barrier to the rate-limiting species.

One of the most interesting results observed in this study is the sharp drop of GRCop-84 oxidation rates in oxygen below ~750 °C. It is a significant departure from the behavior of Cu and NARloy-Z. Another way to state that observation is that, in going from high to intermediate temperatures, the rates of GRCop-84 oxidation exhibit a discontinuous and substantial drop in air and oxygen, the rates for NARloy-Z exhibit some drop in air but not in oxygen, while the rates for Cu oxidation exhibit no discontinuous drop at all. That merely underscores the point that NARloy-Z oxidation behavior is intermediate between those of GRCop-84 and Cu.

The reason for the drop in GRCop-84 oxidation rates is unclear but a few possibilities deserve mention. One relates to the high spatial density of Cr_2Nb precipitates in this alloy. The total precipitate volume fraction in GRCop-84 is 14 percent, but it is very finely dispersed in the Cu matrix, down to nanometer scale, the finer particles being those that form by solid-state precipitation upon cooling of the atomized melt (ref. 5). Such a dispersion of particles can hinder the migration of copper ions across the oxide-substrate interface and thus slow down oxidation kinetics, in a way first postulated by Evans (ref. 13). At high temperatures that effect would be diminished by accelerated diffusion, in agreement with the results presented here. Another explanation concerns the redistribution of Cr, Nb, and Cr_2Nb behind the oxidation front. Elemental analysis by EDS showed a high depletion of these species in the outer oxide scale (figs. 7 and 8), indicating that they are redistributed during oxidation. The poor solubility of Cr and Nb in Cu (ref. 5) and its oxides would make such redistribution sluggish, perhaps sluggish enough to replace Cu diffusion as the rate-limiting step. Whatever the cause of it, the enhanced oxidation resistance of GRCop-84 (over Cu and NARloy-Z) at intermediate temperatures will be a significant advantage in RLV applications.

SUMMARY AND CONCLUSION

GRCop-84 and NARloy-Z behave similarly in air oxidation; however, in O_2 GRCop-84 oxidizes more slowly than NARloy-Z at temperatures below ~750 °C. Therefore, in that regard, GRCop-84 has a substantial advantage over NARloy-Z. However, that advantage is lost at higher temperatures. Hence, a protective coating will be required if GRCop-84 is to be used for RLV combustion chamber liners.

FUTURE WORK

A broad spectrum of studies in GRCop-84 blanching is already underway, involving oxidation-reduction cycling, fire tests in O_2-H_2 cells, and TGA exposures. Further TGA studies will seek to determine why GRCop-84 oxidation rates drop significantly below ~750 °C, how that advantage may be extended to higher temperatures, and whether it is affected by substrate microstructure (e.g. Cr_2Nb precipitate fraction and distribution).

REFERENCES

1. D.L. Ellis, G.M. Michal, and N.W. Orth: *Scripta Met.* **24** (1990) 885.
2. D.L. Ellis, R.L. Dreshfield, M.J. Verrilli, and D.J. Ulmer: "Mechanical Properties of a Cu-8Cr-4Nb Alloy," Earth-to-Orbit Conf., NASA-MSFC, Huntsville, AL, May 1994.
3. D.L. Ellis and D.J. Keller: "Thermophysical Properties of GRCop-84" (to be published).
4. D.L. Ellis, G.M. Michal, and R.L. Dreshfield: "A New Cu-8Cr-4Nb Alloy for High Temperature Applications," *NASA Tech. Memo.* 106910, June 1995.
5. K.R. Anderson: "Effects of Thermal & Mechanical Processing on Microstructures & Desired Properties of Particle-Strengthened Cu-Cr-Nb Alloys," NASA CR—2000-209812, February 2000.
6. D.L. Ellis and H. Yun: "Progress Report on Development of a Cu-8Cr-4Nb Alloy database for the Reusable Launch Vehicle, RLV" (to be published).
7. D. Morgan, J. Franklin, A. Kobayashi, and T. Nguyentat: "Investigation of Copper Alloy Combustion Chamber Degradation by Blanching," Proceedings of Advanced Earth-to-Orbit Propulsion Technology Conference, vol. 2 (1988) 506.

8. M. Murphy, R.E. Anderson, A. Kobayashi, and J.A. Van-Kleeck: Effect of Oxygen/Hydrogen Combustion Chamber Environment on Copper Alloys," Proceedings of Advanced Earth-to-Orbit Propulsion Technology Conference, vol. **2** (1986) 580.
9. K.T. Chiang: *Surface and Coatings Tech.*, 76–77 (1995) 14.
10. K.T. Chiang, T.A. Wallace, and R.K. Clark: *Surface and Coatings Tech.*, **86–87** (1996) 48.
11. J.–H. Park, and K. Natesan: Oxidation of Metals, vol. **39**, Nos. 5/6 (1993) 411.
12. A. Ronnquist and H. Fischmeister: J. Inst. of Metals, vol. 89 (1960) 65.
13. U.R. Evans: J. Electrochem. Soc., **91** (1947) 547.

TABLE I.—OXIDES FOUND (BY XRD) ON Cu8Cr4Nb AFTER 50 HRS TGA IN O_2

Temperature, °C	Whole sample	Oxide scale removed from sample		
		Scale, from top	Scale, from bottom	Substrate, from top
600	CuO Cu_2O Cu			(Oxide could not be removed neatly for XRD)
650		CuO Cu_2O	Cu_2O $CuNb_2O_6$ (probable) $CuCrO_2$ (possible) CrO_2 (possible)	(Oxide could not be removed neatly for XRD)
[a]750		CuO Cu_2O		
800	CuO Cu_2O		$CrNbO_4$ $CuCrO_4$ $CuNb_2O_6$	$CrNbO_4$ $CuCrO_2$ $CuNb_2O_6$ Cr_2O_3 (possible) Cu
850		CuO Cu_2O (minor)	$CrNbO_4$ $CuCrO_4$ $CuNb_2O_6$	$CrNbO_4$ $CuCrO_2$ Cr_2O_3 (probable) Cu
875	CuO Cu_2O		$CrNbO_4$ [b]Unidentified oxide	$CrNbO_4$ [b]Unidentified oxide Cr_2O_3 (probable) Cu
900	CuO Cu_2O		Cu_2O (probable) $CuCrO_2$ (probable)	$CrNbO_4$ Cr_2O_3 (probable) Cu

[a]Wafer, completely converted to oxide.
[b]Spinel structure (a_0 = 8.05) indicated.

TABLE II.—OXIDES FOUND (BY XRD) ON Cu8Cr4Nb AFTER 0.05 to 5.0 HRS TGA IN O_2 at 800 °C

Duration, hr	Top of oxide	Bottom of oxide	Substrate, from top
0.5	CuO Cu_2O	CuO Cu_2O	CuO Cu_2O $CuNb_2O_6$ $CuCrO_2$ (probable) $CrNbO_4$ (probable) Cu
1.0	CuO Cu_2O	CuO $CuCrO_2$ (probable) $CuNb_2O_6$ (probable) $CrNbO_4$ (probable)	 $CuCrO_2$ (probable) $CuNb_2O_6$ (probable) $CrNbO_4$ (probable) Cu
2.0	Cu_2O	CuO $CuNb_2O_6$ (probable) $CuCrO_2$ (possible)	$CuNb_2O_6$ $CuCrO_2$ (probable) $CrNbO_4$ (probable)
3.0	CuO Cu_2O Cu (very minor)	[Oxide film did not spall off the substrate]	
5.0	CuO Cu_2O	Cu_2O $CuNb_2O_6$ $CuCrO_2$	$CuNb_2O_6$ $CuCrO_2$ $CrNbO_4$ Cu

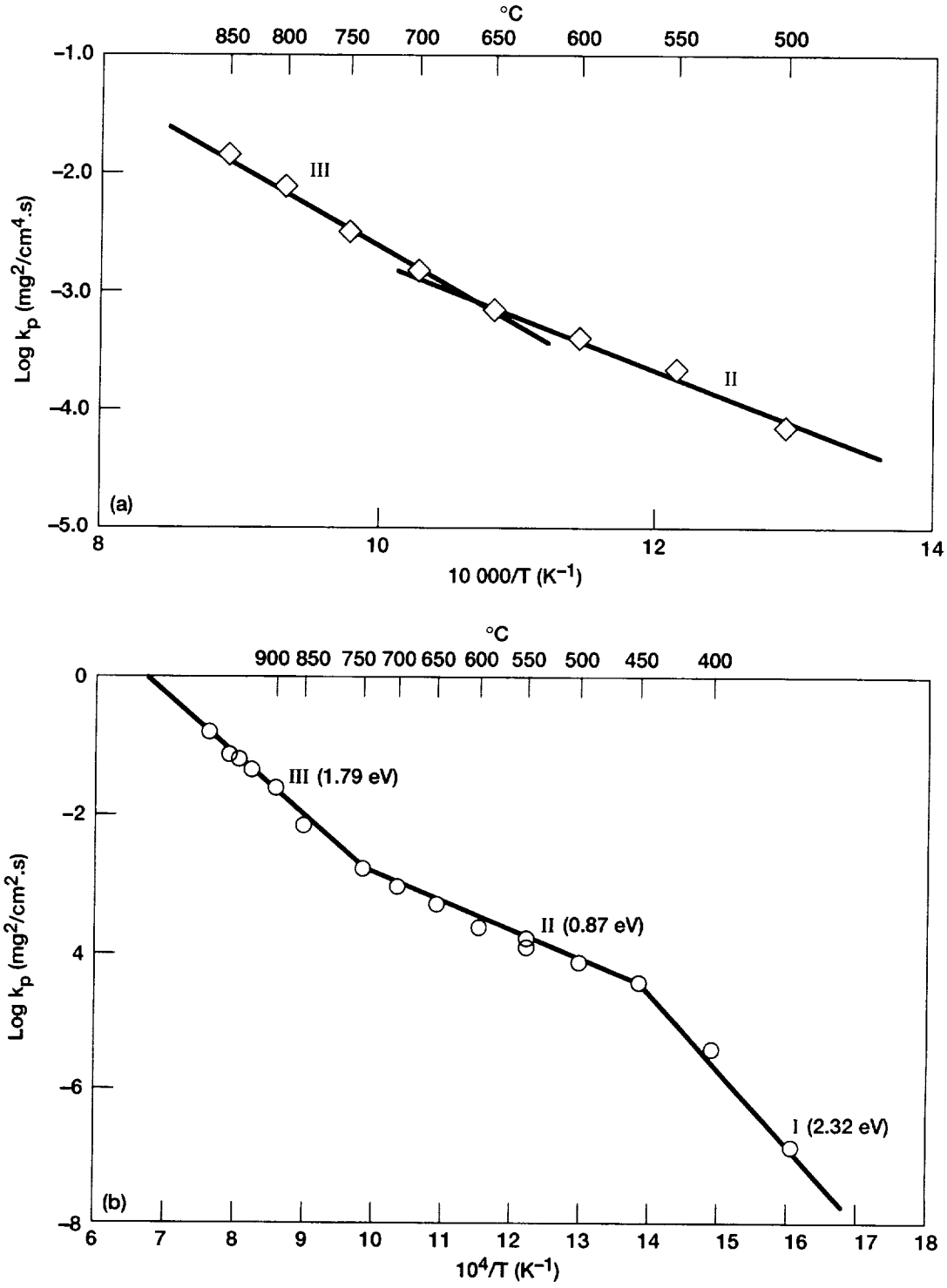

Figure 1.—Oxidation kinetics of pure copper in the low (I), intermediate (II), and high (III) temperature regimes: (a) this study, (b) from ref. II.

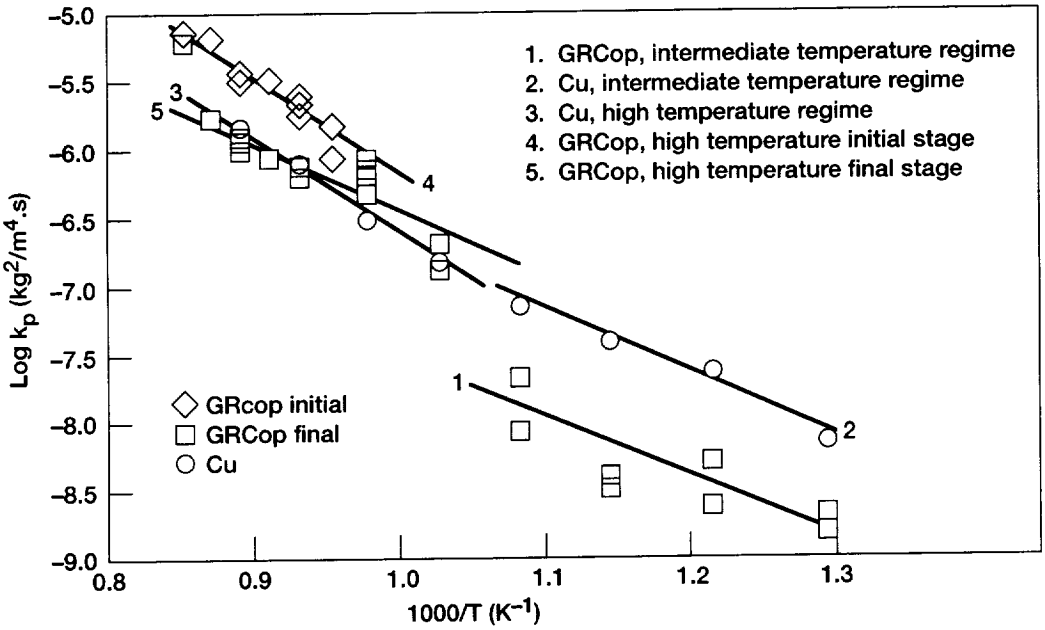

Figure 2.—Oxidation kinetics of GRCop-84 and copper at intermediate and high temperatures. The labeled lines are least-squares regression of data for the corresponding regimes.

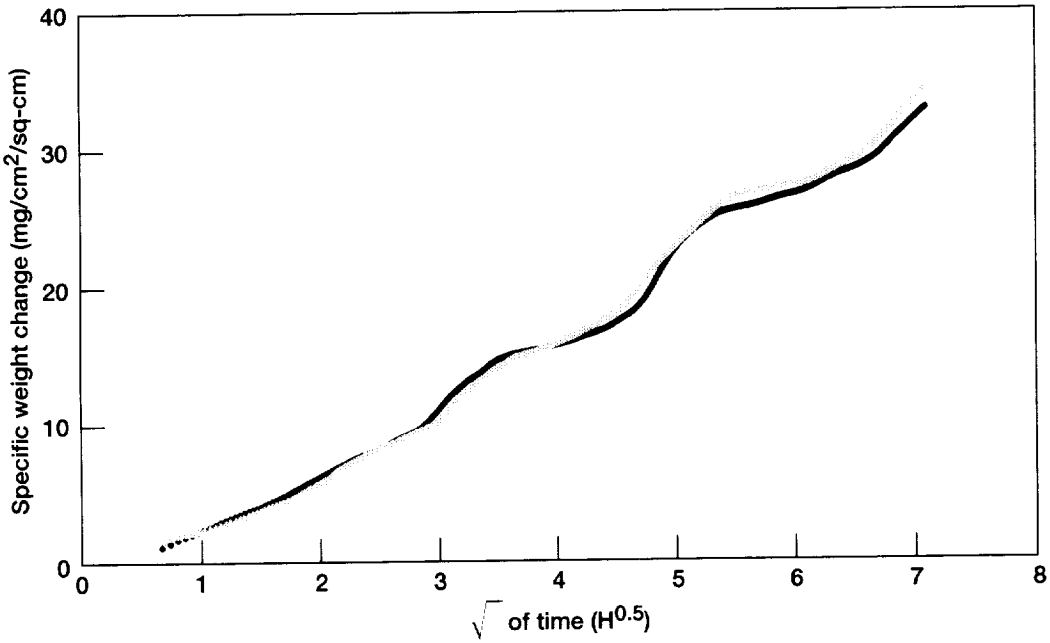

Figure 3.—Unsteady oxidation kinetics of GRCop-84 confirmed by repeat experiments at 750 °C.

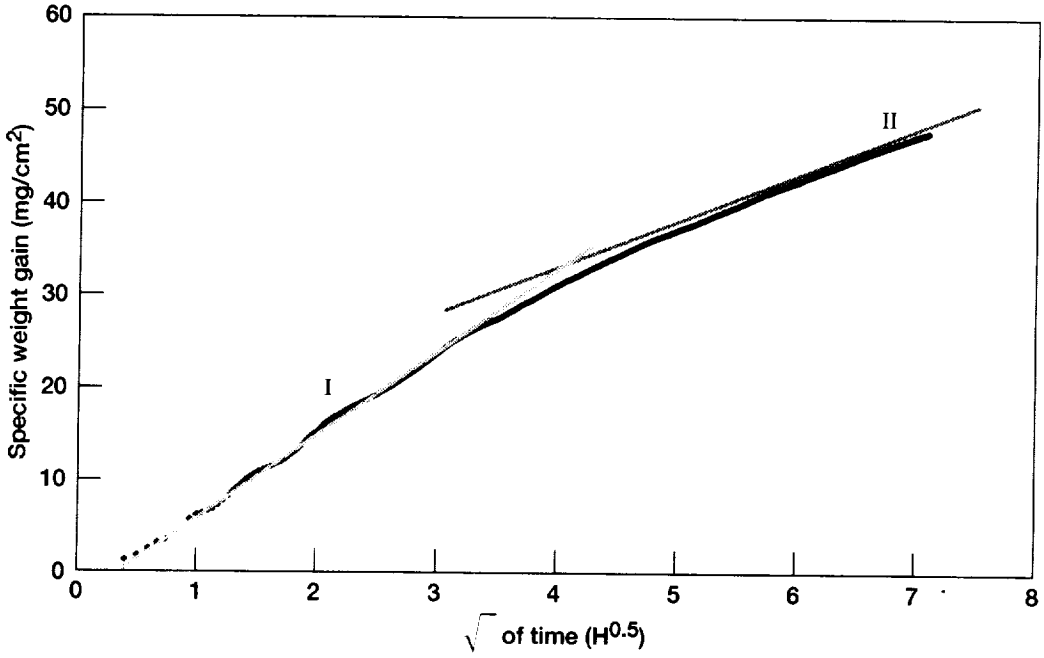

Figure 4.—Parabolic plot of GRCop-84 oxidation in oxygen at 800 °C. The initial- and terminal-stage regions of parabolic behavior are labeled I and II, respectively. The ratio of parabolic rate constants in the two regions, $k_p(I)/k_p(II)$, averaged 3.0 for all temperatures studied.

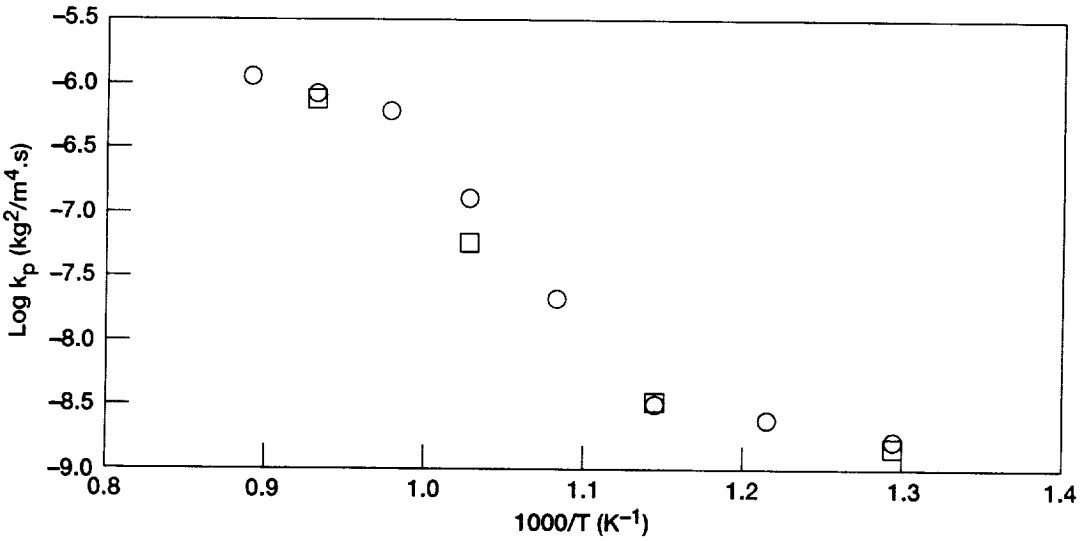

Figure 5.—Comparison of GRCop-84 oxidation behavior in air (squares) and in oxygen (circles) at intermediate and high temperatures. Parabolic rate constants are lower than those at high temperatures by more than two orders of magnitude.

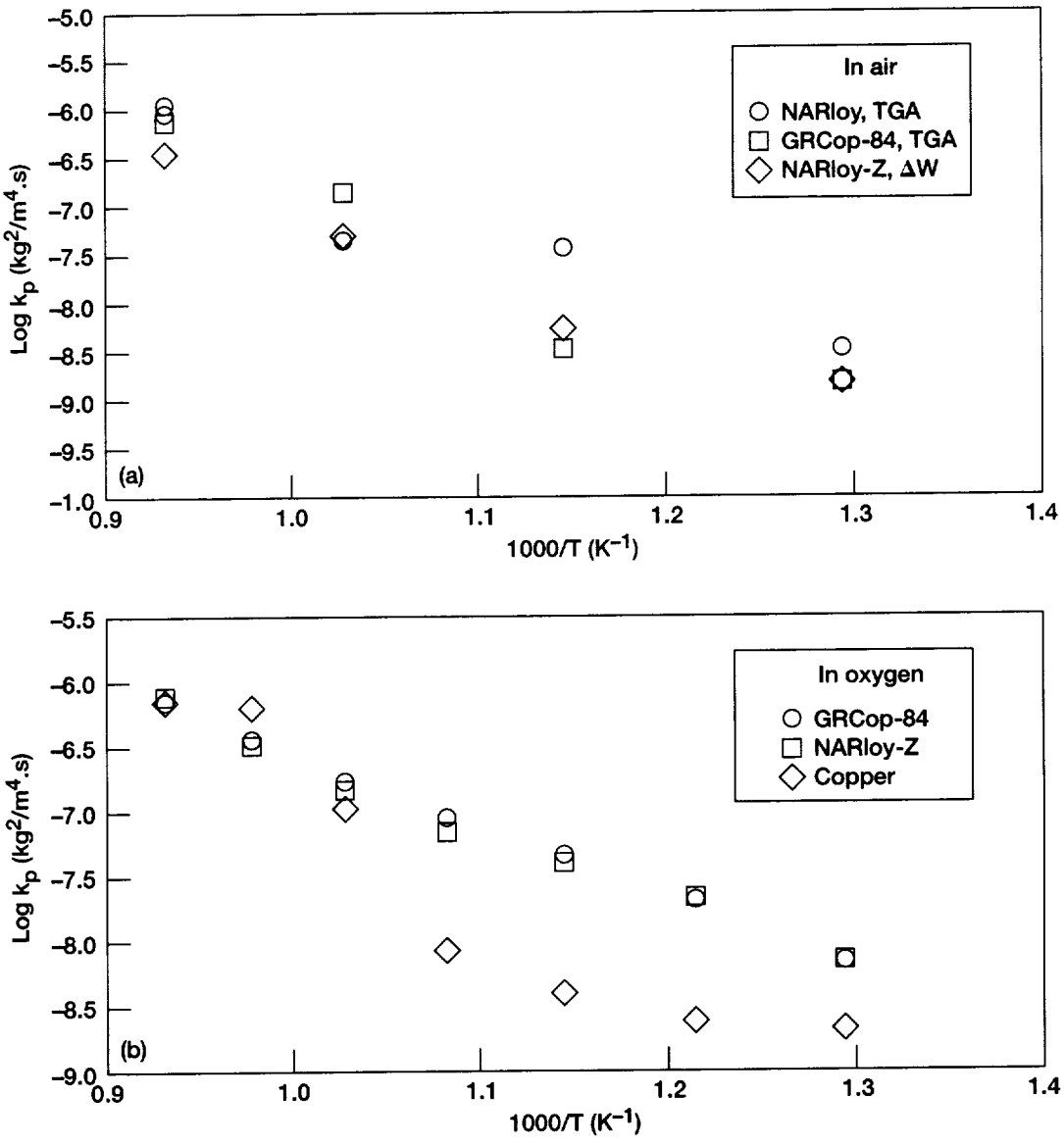

Figure 6.—Comparison of GRCop-84 and NARloy-Z oxidation behavior at intermediate and high temperatures: (a) in air, (b) in oxygen.

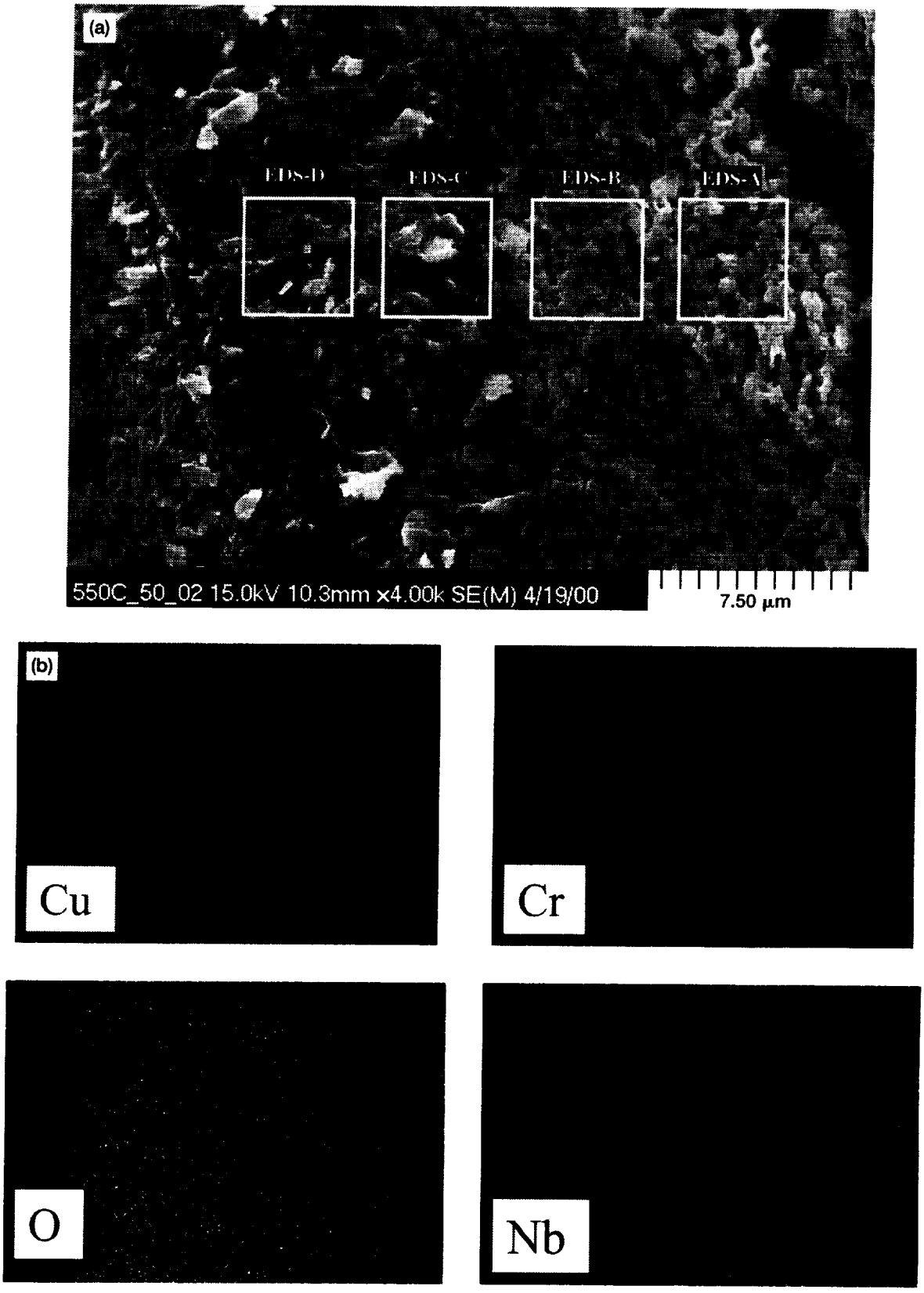

Figure 7.—SEM image (a) and EDS elemental map (b) of oxide grown on GRCop-84 after 50 hrs at 550 °C: Clearly, oxygen is associated with copper, and niobium with chromium.

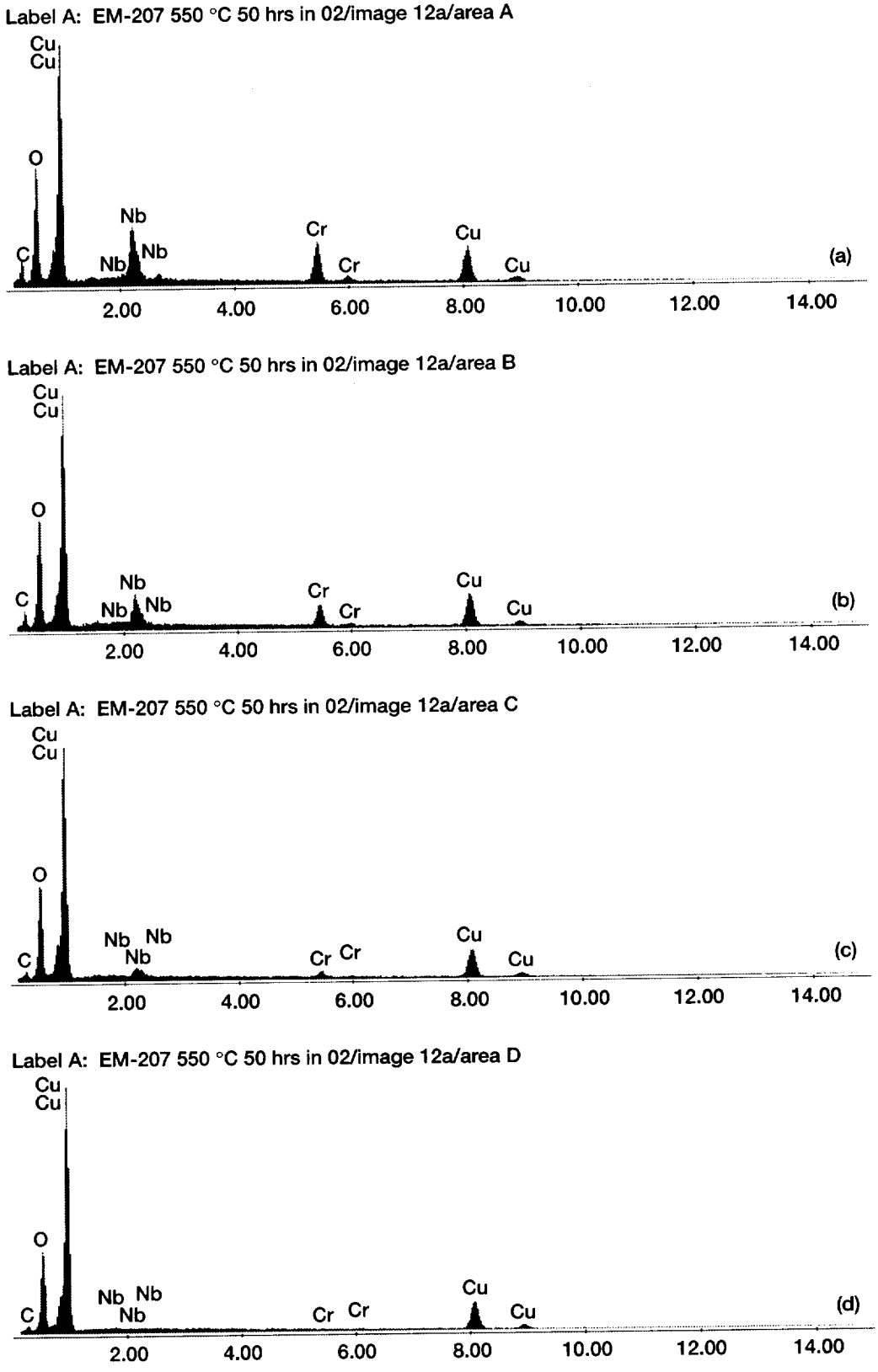

Figure 8.—EDS spectra obtained from the respective areas A-D in Fig. 7 (a), confirming the elemental distribution shown in Fig. 7 (b).

REPORT DOCUMENTATION PAGE

Form Approved
OMB No. 0704-0188

1. AGENCY USE ONLY (*Leave blank*)	2. REPORT DATE	3. REPORT TYPE AND DATES COVERED
	August 2000	Final Contractor Report

4. TITLE AND SUBTITLE

Oxidation Behavior of GRCop-84 (Cu-8Cr-4Nb) at Intermediate and High Temperatures

5. FUNDING NUMBERS

WU–523–61–13–00
NAS3–98008

6. AUTHOR(S)

Linus U. Thomas-Ogbuji and Donald L. Humphrey

7. PERFORMING ORGANIZATION NAME(S) AND ADDRESS(ES)

Dynacs Engineering Company, Inc.
2001 Aerospace Parkway
Brook Park, Ohio 44142

8. PERFORMING ORGANIZATION REPORT NUMBER

E–12420

9. SPONSORING/MONITORING AGENCY NAME(S) AND ADDRESS(ES)

National Aeronautics and Space Administration
Washington, DC 20546–0001

10. SPONSORING/MONITORING AGENCY REPORT NUMBER

NASA CR—2000-210369

11. SUPPLEMENTARY NOTES

Project Manager, Leslie Greenbauer-Seng, Materials Division, NASA Glenn Research Center, organization code 5160, (216) 433–6781.

12a. DISTRIBUTION/AVAILABILITY STATEMENT

Unclassified - Unlimited
Subject Category: 26 Distribution: Nonstandard

This publication is available from the NASA Center for AeroSpace Information, (301) 621–0390.

12b. DISTRIBUTION CODE

13. ABSTRACT (*Maximum 200 words*)

The oxidation behavior of GRCop-84 (Cu-8 at.%Cr-4 at.%Nb) has been investigated in air and in oxygen, for durations of 0.5 to 50 hr and temperatures ranging from 500 to 900 °C. For comparison, data was also obtained for the oxidation of Cu and NARloy-Z (Cu-3 wt.% Ag-0.5 wt.% Zr) under the same conditions. Arrhenius plots of those data showed that all three materials had similar oxidation rates at high temperatures (≥750 °C). However, at intermediate temperatures (500 to 750 °C) GRCop exhibited significantly higher oxidation resistance than Cu and NARloy-Z. The oxidation kinetics of GRCop-84 exhibited a sharp and discontinuous jump between the two regimes. Also, in the high temperature regime GRCop-84 oxidation rate was found to change from a high initial value to a significantly smaller terminal value at each temperature, with progress of oxidation; the two different oxidation rates were found to correlate with a porous intial oxide and a dense final oxide, respectively.

14. SUBJECT TERMS	15. NUMBER OF PAGES
Copper; Alloys; Oxidation; Blanching; Mechanism	17
	16. PRICE CODE A03

17. SECURITY CLASSIFICATION OF REPORT	18. SECURITY CLASSIFICATION OF THIS PAGE	19. SECURITY CLASSIFICATION OF ABSTRACT	20. LIMITATION OF ABSTRACT
Unclassified	Unclassified	Unclassified	

ERRATA

NASA/CR—2000-210369

OXIDATION BEHAVIOR OF GRCop-84 (Cu-8Cr-4Nb) AT INTERMEDIATE AND HIGH TEMPERATURES

Linus U. Thomas-Ogbuji and Donald L. Humphrey

August 2000

Page 9: Replace figure 6 with the figure below. Note that the symbols have been changed in the key in figure 6(b).

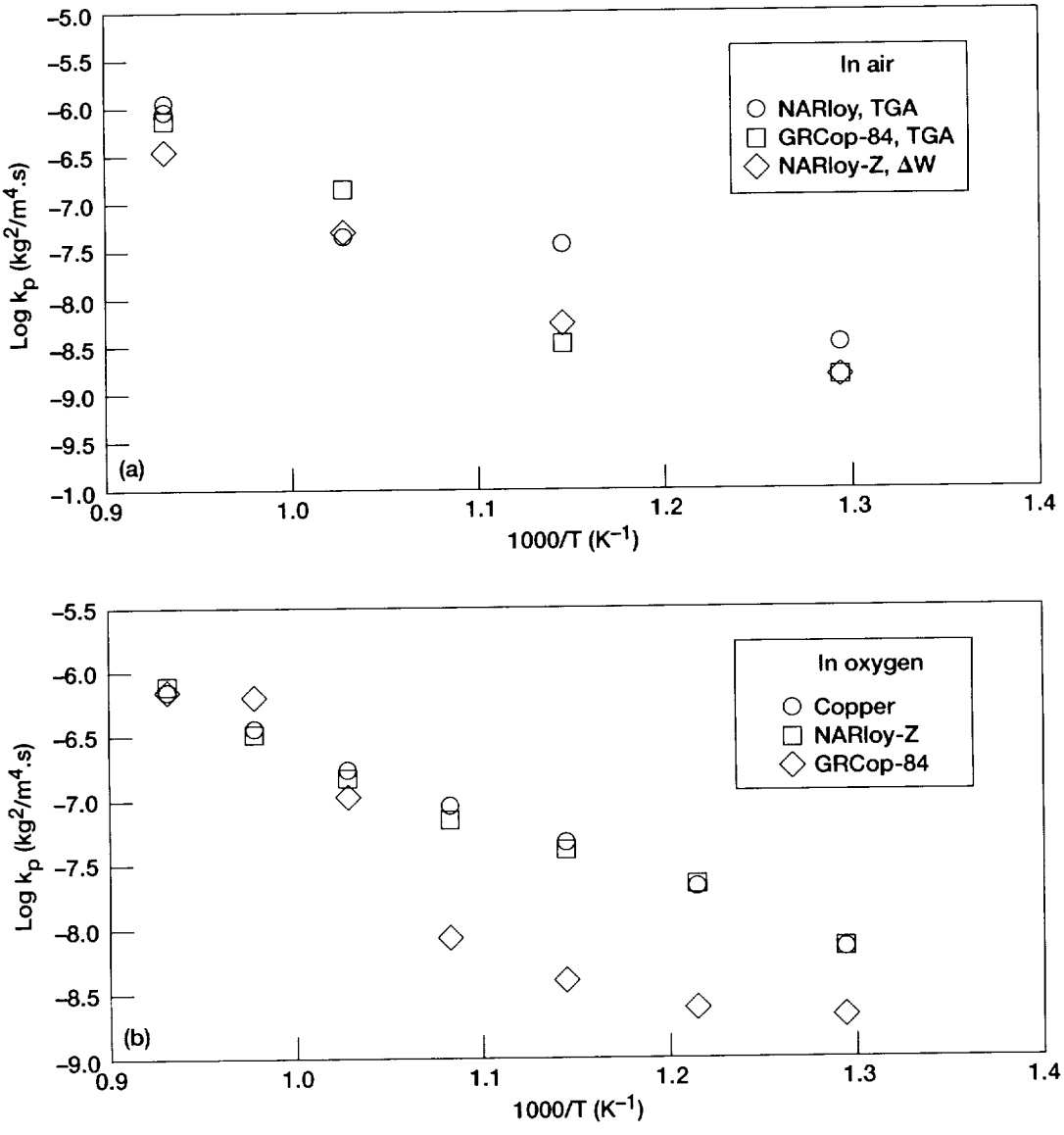

Figure 6.—Comparison of GRCop-84 and NARloy-Z oxidation behavior at intermediate and high temperatures: (a) in air, (b) in oxygen.